Numerical investigation of dense gas flows through transcritical multistage axial Organic Rankine Cycle turbines

L. Sciacovelli[a], P. Cinnella[a]

a. *Laboratoire DynFluid, Arts et Métiers ParisTech, 151 Bd de l'Hôpital, 75013 Paris, France*

Résumé :

Des études récentes suggèrent que les cycles de Rankine organiques supercritiques ont un grand potentiel pour les applications de récupération de chaleur à basse température, car ils permettent d'atteindre une meilleure rendement de récupération avec une architecture de cycle simplifiée. Dans ce travail, on étudie des écoulements de gaz denses à travers des turbines ORC axiales multi-étagées supercritiques, à l'aide d'un code numérique includant des lois d'état complexes et un schéma de discrétisation d'ordre élevé. Plusieurs fluides de travail sont pris en compte et les performances des turbines supercritiques sont comparées à celles de turbines subcritiques utilisant les mêmes fluides.

Abstract :

Many recent studies suggest that supercritical Organic Rankine Cycles have a great potential for low-temperature heat recovery applications, since they allow better recovery efficiency for a simplified cycle architecture. In this work we investigate flows of dense gases through axial, multi-stage, supercritical ORC turbines, using a numerical code including advanced equations of state and a high-order discretization scheme. Several working fluids are considered, and performances of supercritical turbines are compared to those of subcritical ones using the same fluids.

Mots clefs : **ORC turbine ; dense gas ; supercritical fluid**

1 Introduction

Organic Rankine Cycles (ORCs) are Rankine cycles using an organic fluid instead of water working fluid. ORCs have been largely studied for their relatively high efficiency [9] at such unfavorable conditions. ORC technology has been applied in geothermal [11] and biomass [4] fired power plants, bottoming cycles for combined cycle power plants [5], solar reverse osmosis desalination plants, and others, allowing efficiency improvements, reduction of the cycle size and production in modular units. Many studies have demonstrated that supercritical ORCs, i.e., ORCs in which heat is supplied at a pressure greater than the liquid/vapor critical point pressure, have an even greater potential, since they allow better recovery efficiency for a simplified cycle architecture [6]. The selection of the most suitable working fluid is of crucial importance in designing an ORC process, since it requires to take into account thermodynamic, environmental and safety aspects [8].

In this work, we investigate supercritical flows of dense gases/vapors through axial, multi-stage, ORC turbines, using a numerical code with a high-order discretization scheme. Three working fluids are considered : the refrigerants R134a and R245fa, and carbon dioxide (CO_2). The two organic fluids are characterized by complex molecules and moderate to high molecular weights, and can be classified as dense gases according to Cramer and Kluwick [3]. At this stage, we restrict our attention to inviscid flow effects related to the peculiar thermodynamic behavior of each fluid. In most cases, the thermodynamic working conditions of these gases are such that the ideal-gas approximation is no longer valid and real-gas effects become significant. For this reason, an advanced multiparameter equation of state

is required to model the fluids. Hereafter, we first briefly recall the governing equations and thermodynamic models in use, then we describe the ORC turbines under investigation, compare the different flow behaviors obtained with different working fluids, and comment on entropy losses associated to shock wave formation as a function of fluid complexity.

2 Governing Equations and Flow solver

Since in this work we are mainly concerned with the impact of thermodynamic properties of fluids on their inviscid flow behavior, we restrict our attention to the Euler equations, written in integral form for a control volume Ω with boundary $\partial\Omega$:

$$\frac{d}{dt}\int_{\Omega} w\, d\Omega + \int_{\partial\Omega} \mathbf{f}\cdot\mathbf{n}\, dS = 0 \tag{1}$$

where $\mathbf{w} = (\rho, \rho\mathbf{v}, \rho\mathbf{E})^T$ is the conservative variable vector, $\mathbf{n}$ is the outer normal to $\partial\Omega$ and $\mathbf{f} = (\rho v, p\bar{\bar{\mathbf{I}}} + \rho\mathbf{v}\mathbf{v}, \rho\mathbf{v}\mathbf{H})^T$ is the flux density ; $\mathbf{v}$ is the velocity vector, E the specific total energy, $H = E + p/\rho$ the specific total enthalpy, p the pressure and $\bar{\bar{\mathbf{I}}}$ the unit tensor. These equations are completed by a thermal and a caloric equation of state :

$$p = p(\rho(\mathbf{w}), T(\mathbf{w})) \qquad \text{and} \qquad e = e(\rho(\mathbf{w}), T(\mathbf{w})) \tag{2}$$

where e is the specific internal energy and T the absolute temperature.

Dynamic behavior of dense gases is governed by the fundamental derivative of Gas Dynamics Γ [13] :

$$\Gamma = 1 + \frac{\rho}{a}\left(\frac{\partial a}{\partial \rho}\right)_s \tag{3}$$

being ρ the density and $a = [-v^2(\partial p/\partial v)_s]^{\frac{1}{2}}$ the speed of sound. Γ represents a measure of the rate of change of the sound speed. According to whether Γ is higher or lower than unity, the flow exhibits different sound-speed variation in isentropic perturbations : when $\Gamma > 1$, a drops in isentropic expansions and grows in isentropic compressions, which is what happens in common fluids ; an opposite behavior is obtained when $\Gamma < 1$. Thermodynamic regions with Γ lower than unity are observed for molecularly complex fluids at temperatures and pressures close to saturation conditions.

The gas response is modeled through equations of state (EOS) based on Helmholtz free energy Φ, which represent the most accurate available models for the fluids of interest in thermodynamic regions close to the critical point and the saturation curves [7]. EOS are written in the form proposed by Setzmann and Wagner [10] : $\Phi(\delta,\tau) = \Phi^0(\delta,\tau) + \Phi^r(\delta,\tau)$. They use a reduced form (variables normalized with critical-point properties) and are composed by an ideal-gas part, Φ^0, function of the ideal-gas isobaric heat capacity, and by a residual term, Φ^r taking into account real-gas corrections.

$$\begin{aligned}\Phi^r(\delta,\tau) = &\sum_{m=1}^{M_1} a_m \delta^{i_m}\tau^{j_m} + \sum_{m=M_1+1}^{M_2} a_m \delta^{i_m}\tau^{j_m}\exp(-\delta^{k_m}) \\ &+ \sum_{m=M_2+1}^{M_3} a_m \delta^{i_m}\tau^{j_m}\exp[-\alpha_m(\delta-\epsilon_m)^2 - \beta_m(\tau-\gamma_m)^2]\end{aligned} \tag{4}$$

where $\delta = \rho/\rho_c$ is the reduced density and $\tau = T_c/T$ is the inverse reduced temperature. The number of polynomial and exponential terms and the values of coefficients and exponents are calibrated from experimental data using an optimization algorithm described in [10] . A in-house flow solver has been equipped with reference EOS available for R134a [14] and CO_2 [12]. For R245fa, no reference EOS is available, thus we adopt the short technical multiparameter EOS proposed by Span and Wagner [7].

The governing equations are discretized using a cell-centered finite volume scheme for structured multi-block meshes of third-order accuracy. The equations are then integrated in time using a four-stage

Runge-Kutta scheme. Local time stepping, implicit residual smoothing and multi-grid acceleration are used in order to drive the solution to the steady state. The accuracy of the numerical solver, already demonstrated in previous works [1, 2], will be not investigated further.

The geometrical configurations under investigations are axial reaction turbines with a variable number of stages according to the working fluid in use. The reaction degree is fixed to 0.5. The rotational speed is fixed at 3000 RPM to allow direct coupling with the alternator. The number of stages and their relative average radius are calculated in the pre-design phase by considering the operating conditions (inlet total conditions, mass flow and pressure ratio), as well as cost and system complexity considerations. A three-stage turbine working with refrigerant R245fa is designed to work at subcritical nominal conditions, and four-stage turbines, designed for supercritical nominal conditions, are used with fluids R134a and CO_2. The blades use the same airfoils for both stator and rotor wheels. Both the subcritical and supercritical turbines were tested by using both R134a and R245fa as the working fluid, to check the impact of different working fluids on the overall performance of a given turbine. The different turbine configurations under investigation are described in Tab. 1. Blade vanes are discretized by C-meshes made of 272x32 cells. Total temperature and pressure are imposed at inlet, static pressure at the outlet, periodicity at upper and lower boundaries, and no-slip at the wall. A mixing plane condition is used at stator/rotor interfaces.

3 Numerical simulation results

For each turbine configuration and each stage, we computed the isentropic efficiency defined as the real-to-ideal static enthalpy jump ratio. In the present 2D inviscid calculations, only losses due to shock waves can be taken into account. Numerical results show that shock waves are generated, at upper surfaces of rotor blades, for some turbine configurations and operating conditions. However, these shocks remain relatively weak, and the associated entropy losses small. Even in the case the flow field is entirely shock-free, the computed efficiencies are slightly lower than unity, because of errors introduced by the numerical approximation of governing equations and boundary conditions.

Fig. 1 shows distributions of relative Mach number, Fundamental Derivative of Gas Dynamics Γ, and sound speed for case SUPR134a. Weak shock waves are created on the suction side of the rotor blades for all stages. Going from the first to the last stage, Γ becomes lower than unity, and the sound speed increases as the expansion proceeds. Since flow velocity grows more slowly than the sound speed, stronger shocks are generated in the first stages where Mach is higher ; this is reflected by stage isentropic efficiencies, which increase as shocks weaken (see Tab. 2). For case SUPR245fa shown in Fig. 2, a similar behavior is observed. Nevertheless, entropy losses are higher than for R134a. In this case, Γ is lower than unity through the entire turbine : as a consequence, the speed of sound increases during the expansion. However, its value in the upstream stages is much lower than in SUPR134a, whereas flow speed is almost the same, so that Mach number is higher and shocks stronger. This results in efficiencies roughly 5% lower than in the SUPR134a case.

For subcritical configurations SUBR134a and SUBR245fa (not shown for brevity), the overall performance is lower. Lower isentropic efficiencies are due to the fact that the computed Γ value is nearly constant and close to unity : the sound speed growth is negligible with respect to the flow speed one, so that Mach number and shock strength increase moving downstream. Performance loss is partly due to the fact that the subcritical turbine is designed for 3 stages instead of 4 ; as a consequence, each stage processes a higher pressure ratio with respect to the supercritical turbine (see Tab. 1). Subcritical turbine efficiencies about 1.5% lower w.r.t. supercritical configurations.

Finally, case SUPCO_2 is shown in Fig. 3. In this case the flow remains always subsonic and no shocks are formed, since carbon dioxide has a sound speed about double than R134a and R245fa. Thus, even if Γ is higher than unity and the speed of sound decreases with fluid expansion, it is still high enough to prevent the flow from becoming supersonic. In the absence of shocks and viscous effects, isentropic efficiencies differ from unity only because of numerical errors. According to these numerical results, CO_2 seems to be the working fluid that offers the highest adiabatic efficiency. Nevertheless, the choice of an optimal working fluid for ORC turbines also involve other kinds of consideration, like economical and safety considerations. For instance, supercritical CO_2 cycles involve pressures of the

order of 80 bar (the inlet pressure being of about 150 bar in this case), which increases fabrication and installation costs. In addition, the high pressure drop per each stage, greater than 20 bar, could lead to significant leakage flows with respect to the organic fluid turbines.

TABLE 1 – Summary of the considered turbine configurations ; β_i are stage pressure ratios, β_tot the total one.

Parameters	SUBR134a	SUBR245fa	SUPR134a	SUPR245fa	$SUPCO_2$
p0 (bar)	10.4	9.5	47.1	46.9	150.5
T0 (K)	315.51	370.15	396.57	450.43	416.21
Stages	3	3	4	4	4
β_1	1.832	1.840	1.703	1.706	1.214
β_2	1.819	1.823	1.630	1.652	1.229
β_3	1.836	1.838	1.596	1.605	1.242
β_4	-	-	1.586	1.593	1.258
β_{tot}	6.118	6.165	7.026	7.208	2.331

TABLE 2 – Adiabatic efficiencies for each stage.

Stage	SUBR134a	SUBR245fa	SUPR134a	SUPR245fa	$SUPCO_2$
1	95.07	92.55	94.63	91.12	98.72
2	94.03	89.59	95.80	91.99	98.27
3	92.94	88.36	95.87	92.45	99.86
4	-	-	98.41	93.62	99.11

4 Conclusions

In this work, dense gas flows through supercritical multistage axial ORC turbines were analyzed by means of a in-house dense gas numerical solver equipped with high-accurate multiparameter equations of state based on Helmholtz free energy and using a high-order finite volume scheme. Calculations were carried out for 3 different supercritical turbine configurations. Two subcritical ORC turbines were also studied for comparison. Steady, inviscid, two-dimensional numerical simulations were carried out in order to evaluate entropy losses associated to shock wave formation in the different cases. Different behaviors were observed according to the working fluid and turbine configuration considered. The Fundamental Derivative of Gas Dynamics Γ was studied to understand and explain differences in the computed results. Shock-wave formation has a crucial impact on the overall performance : carbon dioxide provides an optimal behavior since, because of the high values of the speed of sound in this fluid, the flow field is completely subsonic and no shocks are created. The use of R134a ensures satisfactory adiabatic efficiencies, both for the subcritical and the supercritical configuration, despite the presence of weak shocks at the suction sides of rotor blades, whereas R245fa develops, for the turbine configuration studied, stronger shocks leading to more significant losses. For both fluids, the use of supercritical inlet conditions tends to increase turbine isentropic efficiency for a given pressure ratio since, at high pressures, their thermodynamic behavior significantly deviates from that of a perfect gas, slowing down the increase of the Mach number during turbine expansion, and leading to weaker shocks. In the next future, we plan to take into account viscous and unsteady effects. Also, 3D calculations are planned as future work.

Références

[1] Cinnella, P., Congedo, P.M. 2005 Numerical solver for dense gas flows. *AIAA J.* **43** pp. 2458-61

[2] Cinnella, P., Congedo, P.M. 2005 Aerodynamic performance of transonic Bethe-Zel'dovich-Thompson flows past an airfoil. *AIAA J.* **43** pp. 370-378

[3] Cramer, M.S., and Kluwick, A. 1984 On the propagation of waves exhibiting both positive and negative nonlinearity. *Journal of Fluid Mechanics* **142** pp. 9-37

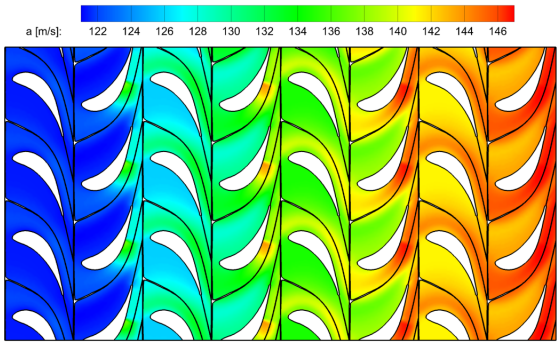

(a) Speed of sound.

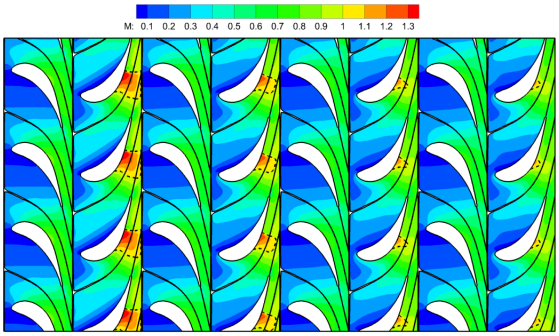

(b) Mach number.

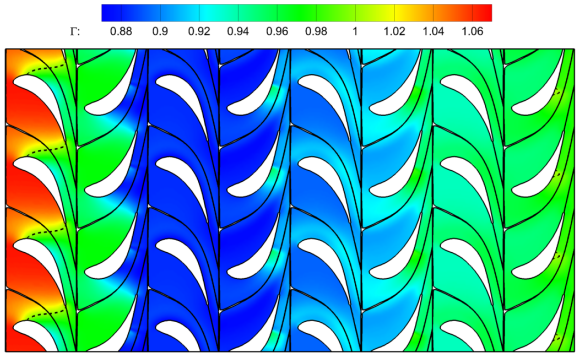

(c) Fundamental Derivative of Gas Dynamics.

FIGURE 1 – Mach, sound speed and Γ contours for case SUPR134a. $M = 1$ and $\Gamma = 1$: – – –.

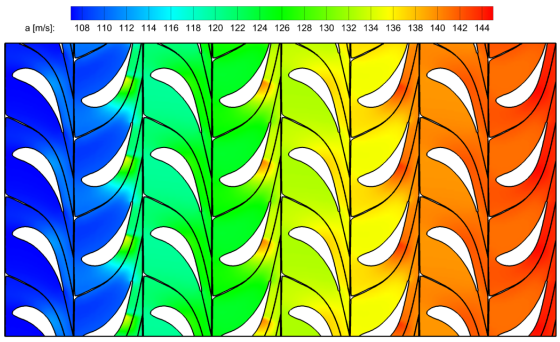

(a) Speed of sound.

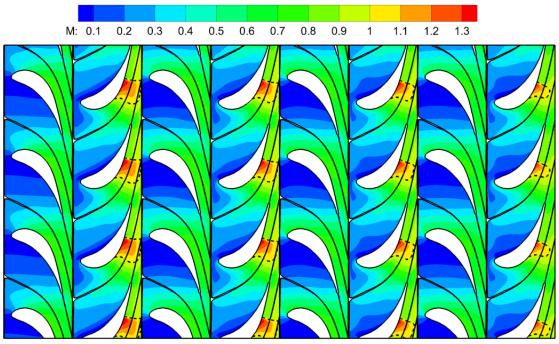

(b) Mach number

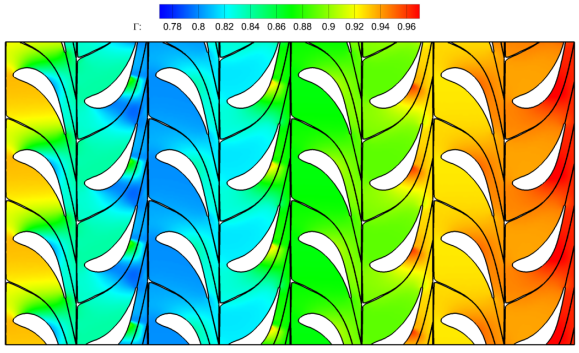

(c) Fundamental Derivative of Gas Dynamics.

FIGURE 2 – Mach, sound speed and Γ contours for case SUPR245fa. $M = 1$: – – –.

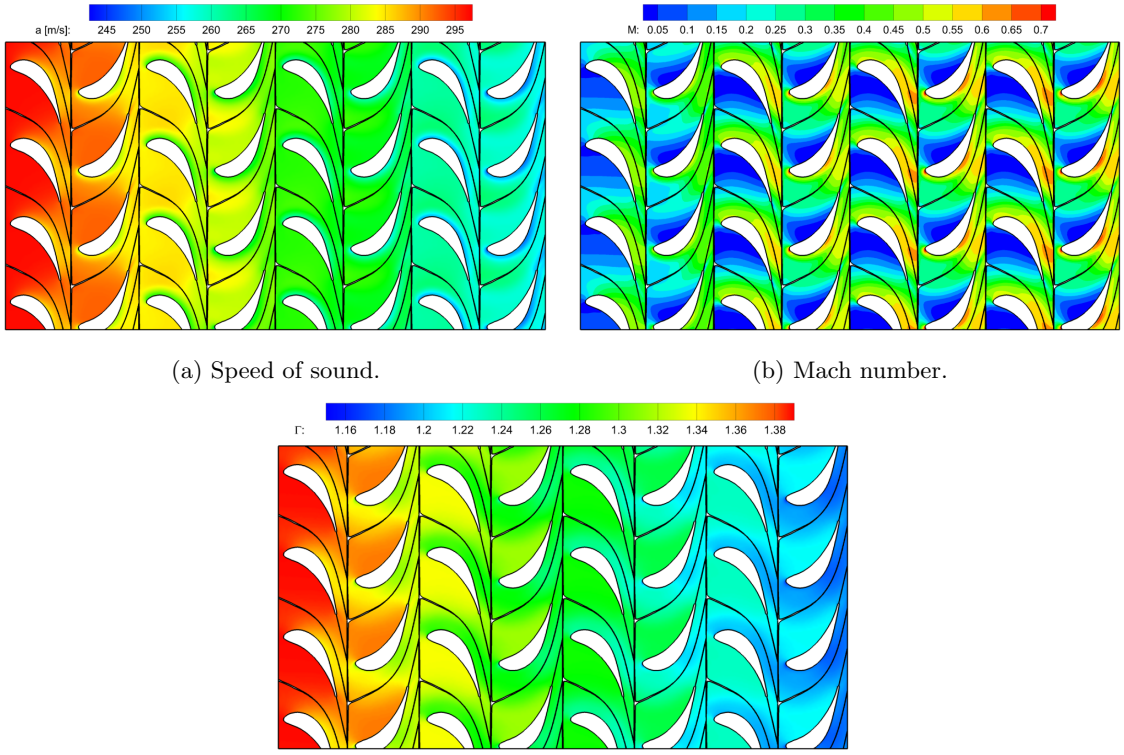

(a) Speed of sound.

(b) Mach number.

(c) Fundamental Derivative of Gas Dynamics.

FIGURE 3 – Mach, sound speed and Γ contours for case SUPCO$_2$.

[4] Drescher, U., Brüuggemann, D. 2007 Fluid Selection for the organic Rankine Cycle (ORC) in biomass power and heat plants.. *Applied Thermal Engineering* **27 (1)** pp. 223-228

[5] Invernizzi, C., Iora, P., Silva, P. 2007 Bottoming micro-Rankine cycles for micro-gas turbines. *Applied Thermal Engineering* **27(1)** pp. 100-110

[6] Karellas, S., Schuster, A. 2010 Supercritical fluid parameters in organic Rankine cycle applications. *Internation Journal of Thermodynamics* **11(3)** pp. 101-108

[7] Lemmon, E.W., Span, R. 2006 Short Fundamental equations of state for 20 industrial fluids. *Journal of Chemical & Engineering Data* **51(3)** pp. 785-850

[8] Liu, B., Chien, K., Wang, S.K. 2004 Effect of working fluids on organic Rankine cycle for waste heat recovery. *Energy* **29(8)** pp. 1207-1217

[9] Schuster, A., Karellas, S., Karakas, E., Spliethoff, H. 2009 Energetic and economic investigation of Organic Rankine Cycle applications. *Appl. Therm. Eng.* **29** pp. 1809-1817

[10] Setzmann, U., and Wagner, W. 1989 A new method for optimizing the structure of thermodynamic correlation equations. *International Journal of Thermophysics* **10** pp. 1103-1126

[11] Shegjun, Z., Huaixin, W., Tao, G. 2011 Performance comparison and parametric optimization of subcritical Organic Rankine Cycle (ORC) and transcritical power cycle system for low-temperature geothermal power generation. *Applied Energy* **88(8)** pp. 2740-2754

[12] Span, R., Wagner, W. 1996 A new equation of state for carbon dioxide covering the fluid region from the triple-point temperature to 1100 K at pressures up to 800 MPa. *Journal of Physical and Chemical Reference Data* **25(6)** pp. 1509-1596

[13] Thompson, P.A. 1971 A Fundamental Derivative in Gas Dynamics. *Physics of Fluids* **14** pp. 1843-1849

[14] Tillner-Roth, R., Baher, H.D. 1994 An international standard formulation for the thermodynamic properties of 1,1,1,2-tetrafluoroehtane (HFC-134a) for temperatures from 170 K to 455 K and pressures up to 70 MPa. *Journal of Physical and Chemical Reference Data* **23(5)** pp. 657-730